

PAPER

Sum Rate Maximization for Multiuser Full-Duplex Wireless Powered Communication Networks

Keigo HIRASHIMA[†], Student Member and Teruyuki MIYAJIMA^{†a)}, Member

SUMMARY In this paper, we consider an orthogonal frequency division multiple access (OFDMA)-based multiuser full-duplex wireless powered communication network (FD WPCN) system with beamforming (BF) at an energy transmitter (ET). The ET performs BF to efficiently transmit energy to multiple users while suppressing interference to an information receiver (IR). Multiple users operating in full-duplex mode harvest energy from the signals sent by the ET while simultaneously transmitting information to the IR using the harvested energy. We analytically demonstrate that the FD WPCN is superior to its half-duplex (HD) WPCN counterpart in the high-SNR regime. We propose a transmitter design method that maximizes the sum rate by determining the BF at the ET, power allocation at both the ET and users, and sub-band allocation. Simulation results show the effectiveness of the proposed method.

key words: wireless energy transfer, energy beamforming, interference suppression, power allocation, sub-band allocation

1. Introduction

With the emergence of Internet-of-Everything systems, large-scale Internet-of-Things (IoT) networks are expected to be developed. Because significant energy resources are required to operate such a large network stably, an energy-efficient communication system is required for 6G systems [1]. For this requirement, wireless energy transmission (WET) via radio frequency (RF) signals is an effective technology to provide energy to energy-constrained communication terminals distributed in a wide area [2]. Simultaneous wireless information and power transfer (SWIPT) systems and wireless powered communication network (WPCN) systems have been actively studied as candidates for WET-based communication systems. In SWIPT, user terminals harvest energy simultaneously while receiving information from RF signals sent by a transmitter. On the other hand, in a WPCN, user terminals harvest energy from RF signals sent by an energy transmitter (ET) and then the user terminals use the harvested energy for wireless information transmission (WIT) to an information receiver (IR) [3].

Most previous studies on WPCN systems assumed half-duplex (HD) transmission based on a harvest-then-transmit protocol, which temporally separates WET and WIT to prevent interference from the ET to the IR [4]–[6]. Several studies have been conducted on transceiver design for HD WPCN systems. In [4], the time allocation for WET and

WIT in a time division multiple access (TDMA)-based multiuser WPCN was optimized by maximizing the sum rate. A joint time and power allocation method that maximizes the energy efficiency of a TDMA-based multiuser WPCN was proposed in [5]. In [6], the beamformer in a space division multiple access (SDMA)-based multiuser WPCN was designed by maximizing the minimum throughput. The major disadvantage of HD WPCN systems is the loss of spectral efficiency because information transmission cannot be performed during the WET phase.

Full-duplex (FD) transmission, which enables simultaneous WET and WIT, is an effective method for overcoming this problem. An inherent problem with FD WPCN systems is that the signal sent by the ET causes interference at the IR, which has a significant negative impact on system performance. The authors of [7] proposed a time allocation method that maximizes the sum rate in a TDMA-based multiuser FD WPCN and demonstrated its superiority over an HD WPCN if the interference can be effectively suppressed. However, specific methods for suppressing the interference were not provided in [7]. In [8], a beamforming (BF) technique at an ET equipped with multiple antennas was employed to suppress the interference in an FD WPCN by directing the null to the IR, demonstrating its effectiveness over an HD WPCN. However, the authors in [8] assumed a single-user system. For large-scale IoT WPCNs, the system should be extended to multiuser systems. In [9], [10], the extensions of the single-user system in [8] to multiuser one were proposed. However, they operate in the HD mode.

Orthogonal frequency division multiple access (OFDMA) has been widely used in narrowband IoT networks to accommodate multiple users because of its low complexity and efficient spectrum utilization [11]. In [12], [13], resource allocation, such as sub-bands and power, for an OFDMA-based WPCN was considered. However, these systems are assumed to operate in the HD mode. The authors in [14] proposed an allocation method for power and sub-bands for an OFDMA-based multiuser FD WPCN with a hybrid access point (HAP), where the ET and IR are collocated and communicate with multiple users. The authors in [15] extend the system in [14] to include relay nodes to support WIT. A HAP equipped with a single antenna transmits the energy signal to the users and simultaneously receives the information signals sent by the users using the harvested energy. Although the IR in the HAP suffers from interference from the ET, concrete methods to suppress it were not provided in [14], [15]. BF at the ET as in [8] is expected to

Manuscript received October 9, 2023.

Manuscript revised January 5, 2024.

Manuscript publicized March 5, 2024.

[†]Graduate School of Science and Engineering, Ibaraki University, Hitachi-shi, 316-8511 Japan.

a) E-mail: teruyuki.miyajima.spc@vc.ibaraki.ac.jp
DOI: 10.23919/transcom.2023EBP3165

effectively mitigate interference even in OFDMA-based FD WPCN systems as in [14], but no such studies have been conducted. This motivates us to study the interference suppression by incorporating BF at the ET into OFDMA-based FD WPCN systems.

In this paper, we consider an OFDMA-based multiuser FD WPCN system with a BF in the ET. In the system, the ET performs BF to efficiently transmit energy to multiple users while suppressing interference to the IR, and the users operating in the FD mode harvest energy from the signals sent by the ET while transmitting information on the allocated sub-bands using the harvested energy to the IR. We propose a transmitter design method that maximizes the sum rate by determining the BF at the ET, power allocated to each sub-band at the ET, sub-bands allocated to each user, and power allocated to each sub-band at each user. Analytical and simulation results are provided to demonstrate the effectiveness of the proposed method.

Throughout this paper, the following notations are used: $(\cdot)^T$, $(\cdot)^H$, and $(\cdot)^*$ indicate the transpose, Hermitian transpose, and complex conjugate of a vector or matrix, respectively. \otimes denotes the Kronecker product, $\mathbf{0}_{N \times M}$ denotes a $N \times M$ matrix whose elements are all zero, \mathbf{I}_N denotes a $N \times N$ identity matrix, $\mathbf{J}_n \in \mathbb{R}^{N \times N}$ denotes a matrix with (n, n) elements of 1 and 0 otherwise, $[x]^+ = \max\{0, x\}$, $|S|$ denotes the number of elements in the set S .

2. System Model

We consider an OFDMA-based FD WPCN system that contains an ET, K users, and an IR (Fig. 1). The ET transmits energy signals toward the users. Each user operating in FD mode harvests energy from its received signal and simultaneously transmits its information data to the IR using the harvested energy. The IR detects the data from its received signal. ET uses M_T transmit antennas to suppress interference to the IR as in the system in [8]. The IR is equipped with a single receiving antenna, and each user is equipped with a single transmitting antenna and a single receiving antenna. We assume that the system has perfect knowledge of all channels, which are frequency-selective. OFDMA with N sub-bands is applied to the energy transmission by the ET and information transmission by the users.

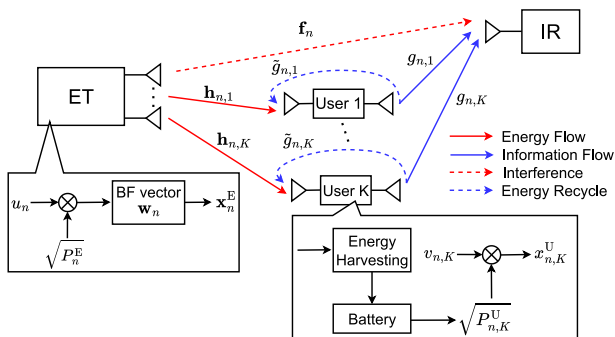


Fig. 1 Proposed OFDMA-based multiuser FD WPCN system.

The transmitted signal of the ET in the n th sub-band is expressed as

$$\mathbf{x}_n^E = \sqrt{P_n^E} \mathbf{w}_n u_n, \quad (1)$$

where P_n^E is the transmit power of the ET in the n th sub-band, $\mathbf{w}_n \in \mathbb{C}^{M_T \times 1}$ is the BF vector in the n th sub-band, and u_n is a random signal for energy transmission in the n th sub-band. We assume that $\{u_n\}$ are normalized and independent of each other, i.e., $\mathbb{E}[u_n u_{n'}^*] = 1$ for $n = n'$, and otherwise 0, and the BF vectors \mathbf{w}_n are normalized, i.e., $\|\mathbf{w}_n\| = 1, \forall n$. Thus, the total transmit power of the ET is given by

$$P^E = \sum_{n=0}^{N-1} \mathbb{E}[\|\mathbf{x}_n^E\|^2] = \sum_{n=0}^{N-1} P_n^E. \quad (2)$$

The transmitted signal from the k th user is expressed as

$$x_{n,k}^U = \sqrt{P_{n,k}^U} v_{n,k}, \quad (3)$$

where $P_{n,k}^U$ is the transmit power of the k th user in the n th sub-band, and $v_{n,k}$ is the data symbol of the k th user in the n th sub-band. We also assume that the transmit symbols $\{v_{n,k}\}$ are normalized and independent of each other, i.e., $\mathbb{E}[v_{n,k} v_{n',k'}^*] = 1$ for $n = n', k = k'$, and otherwise 0. Each user receives the signals sent from the ET and its own transmitted signal owing to the FD operation and harvests energy from the received signals. The harvested power of the k th user is expressed as [12]

$$P_k^{\text{EH}} = \eta \left(\sum_{n=0}^{N-1} P_n^E |\mathbf{h}_{n,k}^T \mathbf{w}_n|^2 + \sum_{n \in \mathcal{N}_k} P_{n,k}^U |\tilde{g}_{n,k}|^2 \right), \quad (4)$$

where $\mathbf{h}_{n,k} \in \mathbb{C}^{M_T \times 1}$ is the channel from the ET to the k th user in the n th sub-band, $\tilde{g}_{n,k} \in \mathbb{C}$ is the loopback channel of the k th user in the n th sub-band, \mathcal{N}_k is the set of the sub-bands allocated to the k th user, and η is the energy conversion efficiency. Note that the users do not suffer from so-called self-interference caused by the FD operation since they do not aim for information reception.

Assuming that each user uses all the harvested energy to transmit its information data, the following relationship holds for all k [†]:

$$\sum_{n \in \mathcal{N}_k} P_{n,k}^U = P_k^{\text{EH}}. \quad (5)$$

Furthermore, from Eqs. (4) and (5), we obtain a closed-form expression for $P_{n,k}^U$ as

$$P_{n,k}^U = \alpha_{n,k} \frac{\eta \sum_{n'=0}^{N-1} P_{n'}^E |\mathbf{h}_{n',k}^T \mathbf{w}_{n'}|^2}{1 - \eta |\tilde{g}_{n,k}|^2}, \quad (6)$$

where a power allocation parameter $\alpha_{n,k} \in \mathbb{R}$ is introduced

[†]Past literature on OFDMA-based WPCNs [12]–[15] imposed an inequality constraint for WIT energy consumption. Instead, we impose the equality constraint, which makes the transmitter design problem tractable.

in place of $P_{n,k}^U$, subject to $\alpha_{n,k} \geq 0$, and $\sum_{n \in \mathcal{N}_k} \alpha_{n,k} = 1$, $\forall k$. We assume that the signals from the ET and all users arriving at the IR are time-aligned within the cyclic-prefix interval. Subsequently, the received signals of the IR in the n th sub-band can be expressed as

$$y_n^I = \sqrt{P_{n,k}^U} g_{n,k} v_{n,k} + \sqrt{P_n^E} \mathbf{f}_n^T \mathbf{w}_n u_n + z_n, \quad (7)$$

where $g_{n,k} \in \mathbb{C}$ is the channel of the k th user in the n th sub-band, $\mathbf{f}_n \in \mathbb{C}^{M_T \times 1}$ is the channel vector from the ET to the IR in the n th sub-band, the first term is the received signal from the k th user in the n th sub-band, the second term is the interference from the ET to the IR in the n th sub-band, and z_n is the additive white Gaussian noise in the n th sub-band at the IR. From Eqs. (6) and (7), the received signal-to-interference-plus-noise ratio (SINR) for the k th user in the n th sub-band at the IR is obtained by

$$\begin{aligned} \gamma_{n,k} &= \frac{P_{n,k}^U |g_{n,k}|^2}{P_n^E |\mathbf{f}_n^T \mathbf{w}_n|^2 + \sigma_z^2} \\ &= \frac{\alpha_{n,k} \sum_{n'=0}^{N-1} P_{n'}^E |\mathbf{h}_{n',k}^T \mathbf{w}_{n'}|^2}{P_n^E |\mathbf{f}_n^T \mathbf{w}_n|^2 + \sigma_z^2} G_{n,k}, \end{aligned} \quad (8)$$

where $G_{n,k} = \frac{\eta |g_{n,k}|^2}{1 - \eta |\hat{g}_{n,k}|^2}$. Note that, according to (5), the SINR includes $\{\mathbf{w}_n\}$ and $\{P_n^E\}$ in both the numerator and denominator. This makes the WET BF design and WET power allocation tractable, as explained in Sect. 4. Subsequently, the achievable sum rate of the system is expressed as

$$R_{\text{sum}} = \sum_{k=1}^K \sum_{n \in \mathcal{N}_k} \log_2(1 + \gamma_{n,k}). \quad (9)$$

The aim of the transmitter design explained in Sect. 4 is to determine the variables $\{\mathbf{w}_n\}$, $\{P_n^E\}$, $\{\alpha_{n,k}\}$, and $\{\mathcal{N}_k\}$ to maximize R_{sum}^\dagger .

3. Performance Analysis

We compare the transmission rate of the FD WPCN with that of the HD WPCN. For simplicity, we assume that the same power $\alpha_{n,k}$ is allocated to all sub-bands in both FD and HD WPCNs and that the sub-bands allocated to a user \mathcal{N}_k are the same for the FD and HD WPCNs. It is reasonable to assume that the harvested power in the HD WPCN is larger than that in the FD WPCN by appropriately setting \mathbf{w}_n and P_n^E because no interference from the ET to the IR exists;

[†]A few sub-bands may be sufficient for the energy transmission and can avoid interference from the ET to the IR. This is valid if there are no restrictions on the power spectral density of the transmitted signals. Even in this case, it is crucial to determine the sub-bands used and appropriate power allocation to the sub-bands for efficient energy transmission. Moreover, it was reported in [16] that it is necessary to distribute the transmit power over multiple sub-bands to comply with regulations such as the power spectral density constraints in the ISM band. These facts justify the power allocation $\{P_n^E\}$ to the sub-bands for the energy transmission.

thus, the BF at the ET can focus only on transmitting energy to users in the HD WPCN.

In the HD WPCN, the users harvest energy from the signals sent by the ET in the first phase of duration τT and send the information data using the harvested energy in the second phase of duration $(1 - \tau)T$, where $0 < \tau < 1$, and T is the block transmission time. Thus, the following relationship between the harvested and transmitted energies of the k th user holds:

$$\tau T P_{\text{EH},k}^{\text{HD}} = (1 - \tau)T \sum_{n \in \mathcal{N}_k} P_{n,k}^U, \quad (10)$$

where $P_{\text{EH},k}^{\text{HD}}$ is the harvested power of the k th HD user. From Eq. (10), we obtain $P_{n,k}^U = \tau P_{\text{EH},k}^{\text{HD}} / (1 - \tau) |\mathcal{N}_k|$ under the assumption of equal power allocation. Therefore, the transmission rate of the k th user in the n th sub-band in the HD WPCN is expressed as

$$R_{n,k}^{\text{HD}} = \log_2 \left(1 + \frac{\tau P_{\text{EH},k}^{\text{HD}} |g_{n,k}|^2}{(1 - \tau) |\mathcal{N}_k| \sigma_z^2} \right), \quad (11)$$

for $n \in \mathcal{N}_k$.

For the FD WPCN, we obtain $P_{n,k}^U = P_{\text{EH},k}^{\text{FD}} / |\mathcal{N}_k|$ under the assumption of equal power allocation, where $P_{\text{EH},k}^{\text{FD}}$ is the power harvested by the k th FD user. Subsequently, the transmission rate of the k th user in the n th sub-band in the FD WPCN is expressed as

$$R_{n,k}^{\text{FD}} = \log_2 \left(1 + \frac{P_{\text{EH},k}^{\text{FD}} |g_{n,k}|^2}{|\mathcal{N}_k| (I_n + \sigma_z^2)} \right), \quad (12)$$

for $n \in \mathcal{N}_k$, where $I_n > 0$ represents the power of the interference from the ET to the IR in the n th sub-band. From the assumption on the harvested power mentioned above, we obtain $P_{\text{EH},k}^{\text{HD}} \geq P_{\text{EH},k}^{\text{FD}} = \mu_k P_{\text{EH},k}^{\text{HD}}$ for $0 \leq \mu_k \leq 1$. In addition, $\sigma_z^2 \leq I_n + \sigma_z^2 = \nu_n \sigma_z^2$ holds for $\nu_n > 1$. Therefore, we can rewrite (12) as $R_{n,k}^{\text{FD}} = \log_2 \left(1 + \mu_k P_{\text{EH},k}^{\text{HD}} |g_{n,k}|^2 / \nu_n |\mathcal{N}_k| \sigma_z^2 \right)$.

By defining the signal-to-noise ratio (SNR) as $\gamma_{n,k} = P_{\text{EH},k}^{\text{HD}} \|g_{n,k}\|^2 / |\mathcal{N}_k| \sigma_z^2$, the transmission rates can be rewritten as

$$R_{n,k}^{\text{HD}} = (1 - \tau) \log_2 \left(1 + \frac{\tau}{1 - \tau} \gamma_{n,k} \right) \quad (13)$$

$$R_{n,k}^{\text{FD}} = \log_2 (1 + \lambda_{n,k} \gamma_{n,k}), \quad (14)$$

where $\lambda_{n,k} = \mu_k / \nu_n$, which satisfies $0 < \lambda_{n,k} < 1$ and indicates the SNR degradation of the FD WPCN. Taking the limit of $\gamma_{n,k} \rightarrow \infty$ for $R_{n,k}^{\text{HD}} / R_{n,k}^{\text{FD}}$, we obtain

$$\begin{aligned} \lim_{\gamma_{n,k} \rightarrow \infty} \frac{R_{n,k}^{\text{HD}}}{R_{n,k}^{\text{FD}}} &= (1 - \tau) \lim_{\gamma_{n,k} \rightarrow \infty} \frac{\log_2(1 + \frac{\tau \gamma_{n,k}}{1 - \tau})}{\log_2(1 + \lambda_{n,k} \gamma_{n,k})} \\ &= 1 - \tau < 1. \end{aligned} \quad (15)$$

The result $R_{n,k}^{\text{FD}} > R_{n,k}^{\text{HD}}$ holds for any k and n . Thus, we can conclude that the sum rate of the FD WPCN is higher

than that of the HD WPCN. Note that, however, the result holds only for a sufficiently high SNR. To evaluate their performance at moderate SNRs, we conducted simulations, which are described in Sect. 5.

4. Transmitter Design

Now, we design the transmitters of the ET and users. Specifically, the problem of determining $\{\mathbf{w}_n\}$, $\{P_n^E\}$, $\{\alpha_{n,k}\}$, $\{\mathcal{N}_k\}$ that maximizes R_{sum} is formulated as follows:

$$(P1): \quad \max_{\{\mathbf{w}_n\}, \{P_n^E\}, \{\alpha_{n,k}\}, \{\mathcal{N}_k\}} R_{\text{sum}} \quad (16)$$

$$\text{s.t.} \quad \|\mathbf{w}_n\| = 1, \forall n, \quad (17)$$

$$\sum_{n=0}^{N-1} P_n^E \leq P_{\text{max}}, \quad (18)$$

$$0 \leq P_n^E \leq P_{\text{peak}}, \forall n, \quad (19)$$

$$\sum_{n \in \mathcal{N}_k} \alpha_{n,k} = 1, \alpha_{n,k} \geq 0, \forall n, k. \quad (20)$$

Equation (18) implies that the total power at the ET is limited to the maximum power P_{max} . Equation (19) implies that the power allocated to each sub-band is limited to the peak power P_{peak} . This is introduced to address power spectral density constraints of transmitted signals [16]. Jointly optimizing problem (P1) for all variables is difficult. Therefore, we consider solving problem (P1) for each variable sequentially.

4.1 Beamforming for Energy Transmission

We consider determining the transmission BF vector $\{\mathbf{w}_n\}$ at the ET when $\{P_n^E\}$, $\{\mathcal{N}_k\}$, and $\{\alpha_{n,k}\}$ are given. We rewrite SINR in (8) as

$$\gamma_{n,k} = \frac{\mathbf{w}^H \tilde{\mathbf{H}}_{n,k} \mathbf{w}}{\mathbf{w}^H \tilde{\mathbf{F}}_n \mathbf{w}}, \quad (21)$$

where $\mathbf{w} = [\mathbf{w}_0^T \dots \mathbf{w}_{N-1}^T]^T \in \mathbb{C}^{M_T N \times 1}$, and $\tilde{\mathbf{H}}_{n,k}$ and $\tilde{\mathbf{F}}_n$ are $M_T N \times M_T N$ block diagonal matrices defined by

$$\tilde{\mathbf{H}}_{n,k} = \alpha_{n,k} G_{n,k} \begin{bmatrix} P_0^E \mathbf{h}_{0,k}^* \mathbf{h}_{0,k}^T & & & \mathbf{0} \\ & \ddots & & \\ & & P_{N-1}^E \mathbf{h}_{N-1,k}^* \mathbf{h}_{N-1,k}^T & \\ \mathbf{0} & & & \end{bmatrix}, \quad (22)$$

$$\tilde{\mathbf{F}}_n = \mathbf{J}_n \otimes P_n^E \mathbf{f}_n^* \mathbf{f}_n^T + \frac{\sigma_z^2}{N} \mathbf{I}_{M_T N}. \quad (23)$$

Assuming a high SINR, the sum rate can be approximated as

$$\begin{aligned} R_{\text{sum}} &\simeq \sum_{k=1}^K \sum_{n \in \mathcal{N}_k} \log_2 \left(\frac{\mathbf{w}^H \tilde{\mathbf{H}}_{n,k} \mathbf{w}}{\mathbf{w}^H \tilde{\mathbf{F}}_n \mathbf{w}} \right) \\ &= \log_2 \left(\prod_{k=1}^K \prod_{n \in \mathcal{N}_k} \frac{\mathbf{w}^H \tilde{\mathbf{H}}_{n,k} \mathbf{w}}{\mathbf{w}^H \tilde{\mathbf{F}}_n \mathbf{w}} \right). \end{aligned} \quad (24)$$

Algorithm 1 GPI Algorithm [17] for Energy BF Design

```

1:  $\kappa = 0$ ,  $\mathbf{w}^{(0)} = \frac{1}{\sqrt{NM_T}} [1, \dots, 1]^T$ 
2: repeat
3:   Compute  $\mathbf{H}(\mathbf{w}^{(\kappa)})$  in (27) and  $\mathbf{F}(\mathbf{w}^{(\kappa)})$  in (28)
4:    $\mathbf{y} = \mathbf{F}(\mathbf{w}^{(\kappa)})^{-1} \mathbf{H}(\mathbf{w}^{(\kappa)}) \mathbf{w}^{(\kappa)}$ 
5:    $\mathbf{w}^{(\kappa+1)} = \mathbf{y} / \|\mathbf{y}\|$ 
6:    $\kappa = \kappa + 1$ 
7: until  $\|\mathbf{w}^{(\kappa)} - \mathbf{w}^{(\kappa-1)}\| < \epsilon$ 
8: for  $n = 0$  to  $N - 1$  do
9:    $\mathbf{w}_n = \frac{\mathbf{J}_n \otimes \mathbf{I}_{M_T} \mathbf{w}^{(\kappa)}}{\|\mathbf{J}_n \otimes \mathbf{I}_{M_T} \mathbf{w}^{(\kappa)}\|}$ 
10: end for

```

Therefore, the optimization problem for determining the BF vector \mathbf{w} that maximizes the sum rate is formulated as

$$(P2): \quad \max_{\mathbf{w}} \prod_{k=1}^K \prod_{n \in \mathcal{N}_k} \frac{\mathbf{w}^H \tilde{\mathbf{H}}_{n,k} \mathbf{w}}{\mathbf{w}^H \tilde{\mathbf{F}}_n \mathbf{w}} \quad \text{s.t.} \quad \|\mathbf{w}\| = N. \quad (25)$$

Problem (P2) can be solved by using a general power iterative (GPI) algorithm [17]. Defining the objective function as $\lambda(\mathbf{w}) = \prod_{k=1}^K \prod_{n \in \mathcal{N}_k} \frac{\mathbf{w}^H \tilde{\mathbf{H}}_{n,k} \mathbf{w}}{\mathbf{w}^H \tilde{\mathbf{F}}_n \mathbf{w}}$, the solutions to problem (P2) should satisfy the condition $\frac{\partial \lambda(\mathbf{w})}{\partial \mathbf{w}^H} = \mathbf{0}$. From the condition, we obtain

$$\mathbf{H}(\mathbf{w}) \mathbf{w} = \lambda(\mathbf{w}) \mathbf{F}(\mathbf{w}) \mathbf{w} \quad (26)$$

where

$$\mathbf{H}(\mathbf{w}) = \sum_{k=1}^K \sum_{n \in \mathcal{N}_k} \left(\prod_{\substack{k=1 \\ i \neq n}}^K \prod_{i \in \mathcal{N}_k} \mathbf{w}^H \tilde{\mathbf{H}}_{i,k} \mathbf{w} \right) \tilde{\mathbf{H}}_{n,k}, \quad (27)$$

$$\mathbf{F}(\mathbf{w}) = \sum_{n=0}^{N-1} \left(\prod_{\substack{i=0 \\ i \neq n}}^{N-1} \mathbf{w}^H \tilde{\mathbf{F}}_i \mathbf{w} \right) \tilde{\mathbf{F}}_n. \quad (28)$$

Because Eq. (26) has a similar form to a generalized eigenvalue problem, we employ the power method, which is an iterative algorithm for solving eigenvalue problems. However, unlike ordinary generalized eigenvalue problems, the matrices in Eq. (26) depend on \mathbf{w} . Therefore, the GPI algorithm updates the matrices during the iterations. The GPI algorithm is summarized in Algorithm 1. In Steps 8 to 10, the BF vector on the n th sub-band is extracted from the resulting vector $\mathbf{w}^{(\kappa)}$ and normalized.

4.2 Power Allocation for Energy Transmission

We consider determining the transmission power $\{P_n^E\}$ at the ET when $\{\mathbf{w}_n\}$, $\{\mathcal{N}_k\}$ and $\{\alpha_{n,k}\}$ are given. The problem of determining $\{P_n^E\}$ that maximizes the sum rate is formulated as

$$\begin{aligned} \max_{P_n^E} \quad & \sum_{k=1}^K \sum_{n \in \mathcal{N}_k} \log_2 \left(1 + \frac{\sum_{n'=0}^{N-1} P_{n'}^E |\mathbf{h}_{n',k}^T \mathbf{w}_n|^2}{P_n^E |\mathbf{f}_n^T \mathbf{w}_n|^2 + \sigma_z^2} \alpha_{n,k} G_{n,k} \right) \\ \text{s.t.} \quad & \sum_{n=0}^{N-1} P_n^E \leq P_{\text{max}}, \quad 0 \leq P_n^E \leq P_{\text{peak}} \quad \forall n, \end{aligned} \quad (29)$$

where $\mathbf{P}_E = [P_0^E \dots P_{N-1}^E]^T$. This problem is difficult to solve because the objective function $R_{\text{sum}}(\mathbf{P}_E)$ is generally nonconvex with respect to \mathbf{P}_E . Hence, to solve this problem as a convex optimization problem, we employ the approach described in [18]. First, the objective function is rewritten as the difference of concave functions as $R_{\text{sum}}(\mathbf{P}_E) = f(\mathbf{P}_E) - g(\mathbf{P}_E)$, where

$$f(\mathbf{P}_E) = \sum_{k=1}^K \sum_{n \in \mathcal{N}_k} \log_2 \left(P_n^E |\mathbf{f}_n^T \mathbf{w}_n|^2 + \sigma_z^2 \right) + \alpha_{n,k} G_{n,k} \sum_{n'=0}^{N-1} P_{n'}^E |\mathbf{h}_{n',k}^T \mathbf{w}_{n'}|^2, \quad (30)$$

$$g(\mathbf{P}_E) = \sum_{n=0}^{N-1} \log_2 \left(P_n^E |\mathbf{f}_n^T \mathbf{w}_n|^2 + \sigma_z^2 \right). \quad (31)$$

Next, the objective function $R_{\text{sum}}(\mathbf{P}_E) = f(\mathbf{P}_E) - g(\mathbf{P}_E)$ is approximated by using a first-order approximation of $g(\mathbf{P}_E)$. Subsequently, the optimization problem is expressed as

$$\begin{aligned} \text{(P3): } \max_{\mathbf{P}_E} & f(\mathbf{P}_E) - g(\mathbf{P}_E^0) - \nabla g^T(\mathbf{P}_E^0) \cdot (\mathbf{P}_E - \mathbf{P}_E^0) \\ \text{s.t. } & \sum_{n=0}^{N-1} P_n^E \leq P_{\text{max}}, 0 \leq P_n^E \leq P_{\text{peak}} \forall n, \end{aligned} \quad (32)$$

where $\mathbf{P}_E^0 \in \mathbb{C}^{N \times 1}$ is any vector satisfying the constraints and

$$\begin{aligned} & \nabla g^T(\mathbf{P}_E) \\ & = \frac{1}{\ln 2} \left[\frac{|\mathbf{f}_0^T \mathbf{w}_0|^2}{P_0^E |\mathbf{f}_0^T \mathbf{w}_0|^2} \dots \frac{|\mathbf{f}_{N-1}^T \mathbf{w}_{N-1}|^2}{P_{N-1}^E |\mathbf{f}_{N-1}^T \mathbf{w}_{N-1}|^2} \right]. \end{aligned} \quad (33)$$

Problem (P3) is concave and solvable via the solver CVXPY [19]. Although an iterative approach that updates \mathbf{P}_E in (32) may provide a better solution, a one-shot solution can provide satisfactory performance according to our preliminary simulation results.

4.3 Power Allocation for Information Transmission

We determine the transmission power allocation parameters $\{\alpha_{n,k}\}$ for users when $\{\mathbf{w}_n\}$, $\{P_n^E\}$, and $\{\mathcal{N}_k\}$ are provided. The problem of determining the allocation parameters $\{\alpha_{n,k}\}$ can be expressed as

$$\begin{aligned} \text{(P4): } \max_{\alpha_{n,k}, \forall n,k} & \sum_{k=1}^K \sum_{n \in \mathcal{N}_k} \log_2 \left(1 + \alpha_{n,k} G'_{n,k} \right) \\ \text{s.t. } & \sum_{n \in \mathcal{N}_k} \alpha_{n,k} = 1, \alpha_{n,k} \geq 0, \forall n, k, \end{aligned} \quad (34)$$

where

$$G'_{n,k} = \frac{\sum_{n'=0}^{N-1} P_{n'}^E |\mathbf{h}_{n',k}^T \mathbf{w}_{n'}|^2}{P_n^E |\mathbf{f}_n^T \mathbf{w}_n|^2 + \sigma_z^2} G_{n,k}. \quad (35)$$

This problem can be solved using the water-filling algorithm. Therefore, the solution of (P4) is given by

$$\alpha_{n,k} = \left[v_k - \frac{1}{G'_{n,k}} \right]^+, \quad n \in \mathcal{N}_k, \quad (36)$$

where the water level v_k is calculated numerically to satisfy the constraints in (P4).

4.4 Sub-Band Allocation for Information Transmission

We consider determining the sub-band allocation $\{\mathcal{N}_k\}$. Because information transmission can be considered an uplink OFDMA transmission, we can exploit the concept of a sub-band allocation algorithm for uplink OFDMA in [20]. The key concept of the algorithm is to allocate the n th sub-band to the k th user with the highest transmission rate as

$$\text{(P5): } k = \arg \max_{k'} \{ \log_2(1 + \alpha_{n,k'} G'_{n,k'}) \}, \quad (37)$$

where the transmission rate $\log_2(1 + \alpha_{n,k'} G'_{n,k'})$ is obtained by allocating all unallocated sub-bands to the k' th user. To adopt criterion (37) in our system, we require further assumptions. To compute the transmission rates, we require $\{\alpha_{n,k}\}$, $\{G'_{n,k}\}$, $\{\mathbf{w}_n\}$ and $\{P_n^E\}$, as shown in (35). Here, we assume that P_n^E are identical for all n . To obtain $\{\mathbf{w}_n\}$, we use Algorithm 1 under the assumption of equal power allocation for $\alpha_{n,k}$. Subsequently, we refine $\{\alpha_{n,k}\}$ using (36) and allocate sub-bands to users based on (37) until all sub-bands are allocated. The resulting algorithm for sub-band allocation is summarized in Algorithm 2.

4.5 Summary of Transmitter Design

The BF design and resource allocation described above are performed according to the following steps.

- Step1) Determine $\{\mathcal{N}_k\}$ using Algorithm 2.
- Step2) Initialize $P_n^E = P_{\text{max}}/N, \alpha_{n,k} = 1/|\mathcal{N}_k| \forall n, k$.

Algorithm 2 Sub-band Allocation Algorithm

- 1: $\mathcal{N} = \{0, 1, \dots, N-1\}, \tilde{\mathcal{N}} = \emptyset, \tilde{\mathcal{N}}_k = \emptyset, \forall k$
 - 2: $P_n^E = P_{\text{max}}/N, \forall n$
 - 3: **for** $k = 1$ to K **do**
 - 4: $\alpha_{n,k} = 1/N, \forall n$
 - 5: Determine $\{\mathbf{w}_{n,k}\}$ using **Algorithm 1**
 - 6: Determine $\{G'_{n,k}\}$ using (35)
 - 7: **end for**
 - 8: **while** $\sum_{k=1}^K |\tilde{\mathcal{N}}_k| = N$ **do**
 - 9: **for** $k = 1$ to K **do**
 - 10: $\mathcal{N}_k = \mathcal{N}, \mathbf{w}_n = \mathbf{w}_{n,k}, \forall n$
 - 11: Determine $\{\alpha_{n,k}\}$ using (36)
 - 12: **end for**
 - 13: **for** $n \in \mathcal{N}$ **do**
 - 14: **if** $r_{n,k} = \log_2(1 + \alpha_{n,k} G'_{n,k}) = 0, \forall k$ **then**
 - 15: $\tilde{\mathcal{N}} = \tilde{\mathcal{N}} + \{n\}$
 - 16: **else**
 - 17: $k = \arg \max_{k'} \{r_{n,k'}\}, \tilde{\mathcal{N}}_k = \tilde{\mathcal{N}}_k + \{n\}$
 - 18: **end if**
 - 19: **end for**
 - 20: $\mathcal{N} = \tilde{\mathcal{N}}, \tilde{\mathcal{N}} = \emptyset$
 - 21: **end while**
 - 22: $\mathcal{N}_k = \tilde{\mathcal{N}}_k$
-

- Step3) Using $\{P_n^E\}, \{\alpha_{n,k}\}, \{\mathcal{N}_k\}$, determine $\{\mathbf{w}_n\}$ using Algorithm 1.
- Step4) Using $\{\mathbf{w}_n\}, \{\alpha_{n,k}\}, \{\mathcal{N}_k\}$, determine $\{P_n^E\}$ by solving (P3).
- Step5) Using $\{\mathbf{w}_n\}, \{P_n^E\}, \{\mathcal{N}_k\}$, determine $\{\alpha_{n,k}\}$ by solving (36).

The computational complexity of Steps 1, 3, 4, and 5 are $O(K(N^2M_T^2 + NM_T^3))$, $O(N^2M_T^2 + NM_T^3)$, $O(N^3)$ [18], and $O(N^2M_T)$, respectively. Note that the proposed design method can only provide suboptimal solutions. However, simulations in the next section validate that the suboptimal solutions can provide satisfactory performances.

5. Simulation Results

We evaluated the performance of the proposed system using computer simulations. Unless otherwise stated, the simulation settings were as follows: The number of subbands was $N = 16$, the number of transmit antennas of the ET was $M_T = 5$, the number of users was $K = 2$, the energy-conversion efficiency was $\eta = 0.6$ [21], the maximum transmit power of the ET was $P_{\max} = 40$ dBm, the maximum transmit power per sub-band of the ET was $P_{\text{peak}} = 8P_{\max}/N$, the loopback gain of the user was -10 dB, the noise power was $\sigma_z^2 = -90$ dBm, the distance attenuation was $(c/4\pi f_c)^2 d^{2.4}$, where c is the speed of light, d is the distance, and the carrier frequency was $f_c = 900$ MHz. The Rayleigh fading channels were modeled as linear FIR filters with a 6 tap exponentially decaying power profile. The locations of the ET, users, and IR are shown in Fig. 2. The ET and IR were located at $(-6\text{ m}, 0\text{ m})$ and $(6\text{ m}, 0\text{ m})$, respectively, and the users were uniformly distributed in a circle with the center $(x_U, 0)$ and radius 3 m . Except for Fig. 8, we set $x_U = 0$. The average sum rates were obtained from 10^3 simulation trials in which each trial had an independent channel realization.

First, we confirmed the convergence of the GPI algorithm because convergence cannot be ensured analytically. Figure 3 shows convergence characteristics for $M_T = 2, 5$, and 10 . The GPI algorithm converged after about 10 iterations for any number of antennas.

Next, we evaluated the performance of the proposed BF method. Figure 4 shows the sum rate characteristics for various BF methods as a function of the number of antennas M_T at the ET. ‘‘EH maximization BF’’ maximized the harvested power in Eq. (4), which was obtained using a normalized eigenvector corresponding to the largest eigenvalue of the matrix derived from (4). ‘‘Interference Nulling BF’’ completely canceled the interference at the IR, i.e., $\mathbf{f}_n^T \mathbf{w}_n = 0$ for $M_T \geq 2$. When no BF was performed (labeled as ‘‘w/o BF’’), we set $\mathbf{w}_n = 1/\sqrt{M_T}[1, \dots, 1]$. For ‘‘w/o BF’’ and ‘‘Interference Nulling BF,’’ the sum rate did not increase as the number of antennas increased because they did not consider the sum rate improvement. For ‘‘EH maximization BF,’’ the sum rate increased as the number of antennas increased. However, owing to the significant influence of interference,

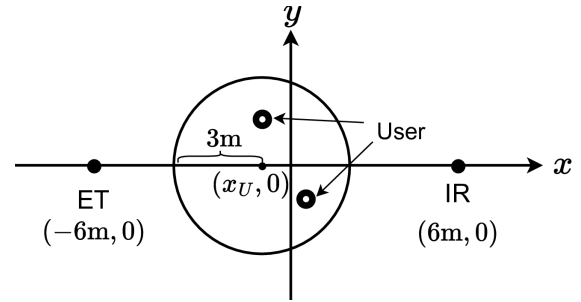


Fig. 2 Locations of ET, IR, and users.

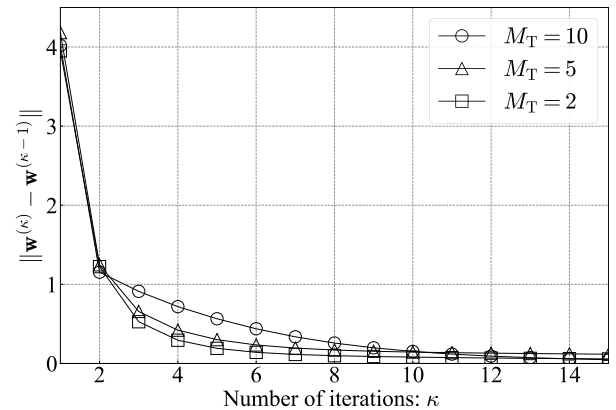


Fig. 3 Convergence characteristics of GPI algorithm.

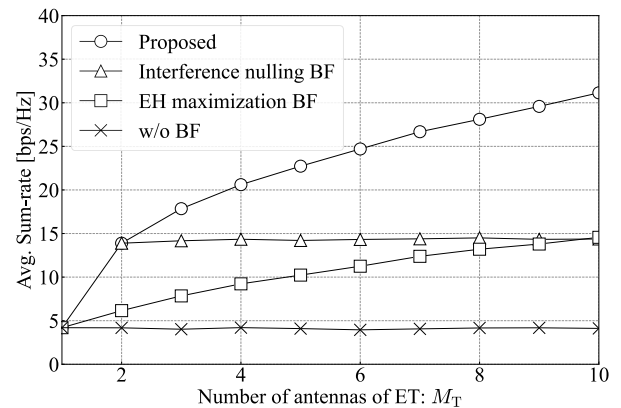


Fig. 4 Performance comparison of the various BF methods.

its performance was not even comparable to that of ‘‘Interference Nulling BF.’’ The proposed method also increased the sum rate as the number of antennas increases and achieved a higher sum rate than the other methods. This is because the proposed method determines BF by considering both interference suppression and efficient energy transmission.

Next, we considered power allocation at both the ET and users. Figure 5 shows the sum rates of the power allocation methods as a function of the maximum transmission power of the ET, where ‘‘Equal Power Allocation’’ was the case in which $P_n^E = P_{\max}/N$ and $\alpha_{n,k} = 1/|\mathcal{N}_k|, \forall n, k$. The sum rates of both methods increased with increasing P_{\max} because the BF at the ET considerably suppressed the interference at

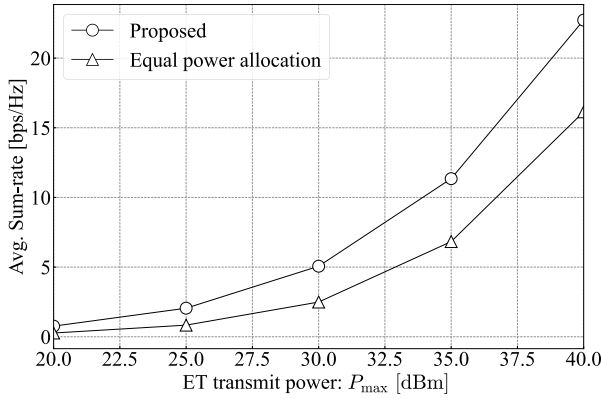


Fig. 5 Performance of power allocation methods.

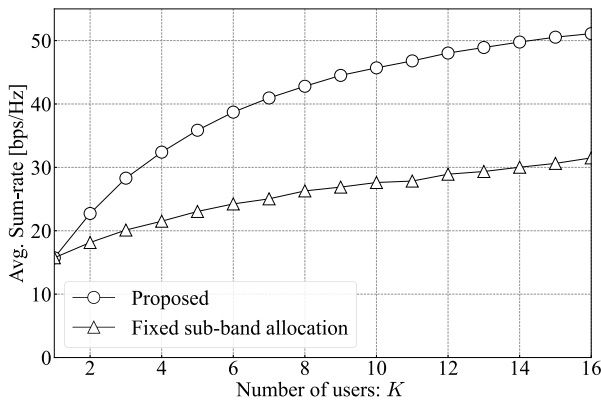


Fig. 6 Performance of sub-band allocation methods.

the IR. The proposed method had a higher rate at any P_{\max} than “Equal Power Allocation” owing to appropriate power allocation.

Next, we considered sub-band allocation methods. Figure 6 shows the sum rate characteristics with respect to the number of the users, where “Fixed Sub-band Allocation” was the case in which the sub-bands allocated to the k th user were $n = (k - 1) + iK, i = 0, 1, \dots, \lfloor N/K - 1 \rfloor$. When $K = 1$, the proposed method was identical to a fixed allocation because no sub-band allocation was performed. The performance difference between the proposed method and fixed allocation increased as the number of users increased. This is because an increase in the number of users provides multi-user diversity, which utilizes combinations of users and sub-bands with favorable channel conditions.

Next, we considered the effect of the transmission power constraint per sub-band at the ET. Figure 7 shows the sum rate characteristics with respect to the transmission power constraint per sub-band P_{peak} , where “Equal Power Allocation at ET” was the case in which $P_n^E = P_{\max}/N$. By increasing P_{peak} , the power could be allocated intensively to a few specific sub-bands as long as the maximum transmit power was not exceeded. The figure shows that the sum rate improvement using the proposed method increased with an increase P_{peak} . This result indicates that to improve the sum rate, a few specific sub-bands, rather than all the sub-bands

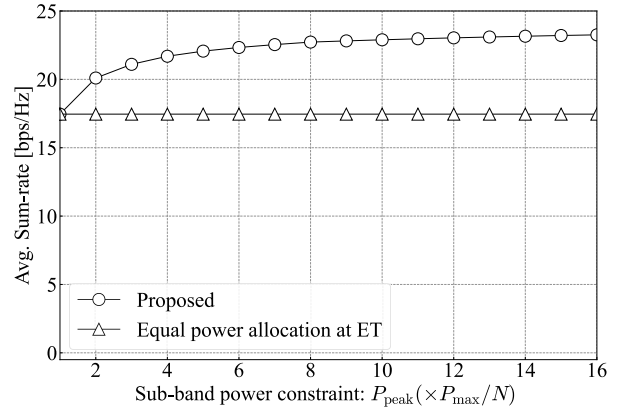


Fig. 7 Effect of transmission power per sub-band at the ET.

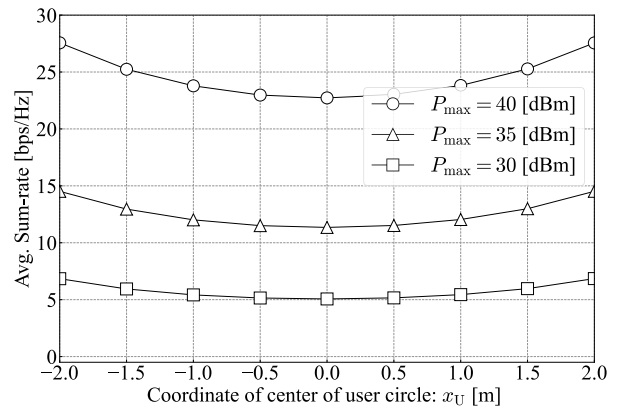


Fig. 8 Effect of user location.

in energy transmission, should be used. However, such a large power allocation to a few sub-bands is not always possible in practical scenarios because it might violate the legal constraints of the transmit power [22].

Next, we considered the effect of the locations of users. Figure 8 shows the sum rates when the x -coordinate x_U of the center of the circle in which the users existed changed. The sum rate had a minimum at $x_U = 0$ and was symmetric around $x_U = 0$ for any P_{\max} . Therefore, it is preferable for users to move toward either ET or IR. This is not the case when using an HAP in which both ET and IR are collocated.

Finally, we compared the proposed FD WPCN with the HD WPCN designed using the proposed method with $\mathbf{f}_n = \mathbf{0}$ and $\tilde{q}_{n,k} = 0$. Figure 9 shows the sum rates as a function of the time allocated for energy transmission τ where the sum rate of the HD WPCN was obtained using $\sum_{k=1}^K \sum_{n \in \mathcal{N}_k} (1 - \tau) \log_2(1 + \frac{\tau}{1-\tau} \gamma_{n,k})$ and $M_T = 2$. Unlike the analytical results for the high-SNR regime in Sect. 3, the transmission rate of the HD WPCN depended on τ because the SNR was not sufficiently high in the simulation setup. The results show that the proposed FD WPCN exhibited a higher sum rate than the HD WPCN, regardless of τ even in the moderate-SNR regime.

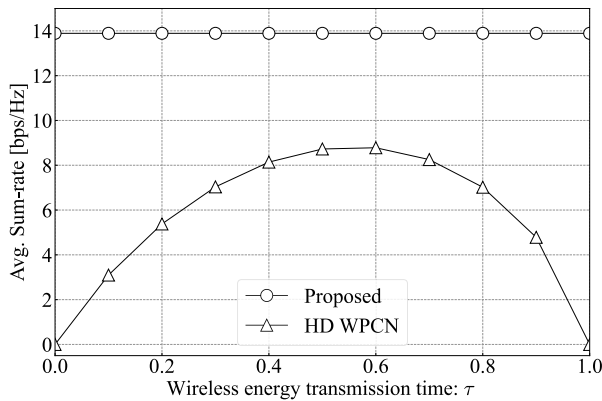


Fig. 9 Comparison with the half-duplex WPCN system.

6. Conclusion

This paper has investigated an OFDMA-based multiuser FD WPCN system with BF. We proposed a sum rate maximization design method that determines the BF and transmit power allocation at the ET, as well as the transmit power and sub-band allocation of each user. The analytical results demonstrated the superiority of the FD WPCN over the HD WPCN in the high-SNR regime. The simulation results showed that the proposed transmitter design is effective in improving the sum rate even in a moderate SNR regime.

Acknowledgments

This study was supported by JSPS KAKENHI (Grant number: JP20K04479, JP24K07472).

References

- [1] D.C. Nguyen, M. Ding, P.N. Pathirana, A. Seneviratne, J. Li, D. Niyato, O. Dobre, and H.V. Poor, "6G Internet of Things: A comprehensive survey," *IEEE Internet Thing J.*, vol.9, no.1, pp.359–386, Jan. 2022.
- [2] X. Lu, P. Wang, D. Niyato, D.I. Kim, and Z. Han, "Wireless charging technologies: Fundamentals, standards, and network applications," *IEEE Commun. Surveys Tuts.*, vol.18, no.2, pp.1413–1452, 2nd Quart. 2016.
- [3] S. Bi, Y. Zeng, and R. Zhang, "Wireless powered communication networks: An overview," *IEEE Wireless Commun.*, vol.23, no.2, pp.10–18, April 2016.
- [4] H. Ju and R. Zhang, "Throughput maximization in wireless powered communication networks," *IEEE Trans. Wireless Commun.*, vol.13, no.1, pp.418–428, Jan. 2014.
- [5] Q. Wu, M. Tao, D.W. K. Ng, W. Chen, and R. Schober, "Energy-efficient transmission for wireless powered multiuser communication networks," *Proc. IEEE Int. Conf. Commun. (ICC)*, London, UK, pp.154–159, June 2015.
- [6] L. Liu, R. Zhang, and K. Chua, "Multi-antenna wireless powered communication with energy beamforming," *IEEE Trans. Commun.*, vol.62, no.12, pp.4349–4361, Dec. 2014.
- [7] H. Ju, K. Chang, and M.-S. Lee, "In-band full-duplex wireless powered communication networks," *Proc. 2015 17th Int. Conf. Adv. Commun. Technol. (ICACT)*, Pyeong Chang, pp.23–27, July 2015.
- [8] Y. Che, J. Xu, L. Duan, and R. Zhang, "Multiantenna wireless powered communication with cochannel energy and information transfer," *IEEE Commun. Lett.*, vol.19, no.12, pp.2266–2269, Dec. 2015.
- [9] M.-L. Ku and C.-Y. Lin, "Beamforming and resource allocation for charging power minimization in multiuser wireless-powered networks," *IEEE Access*, vol.9, pp.136231–136242, 2021.
- [10] J. Choi, C. Song, and J. Joung, "Wireless powered information transfer based on zero-forcing for multiuser MIMO systems," *IEEE Trans. Veh. Technol.*, vol.67, no.9, pp.8561–8570, Sept. 2018.
- [11] A.A. Zaidi, R. Baldemair, V. Moles-Cases, N. He, K. Werner, and A. Cedergren, "OFDM numerology design for 5G new radio to support IoT, eMBB, and MBSFN," *IEEE Commun. Standards Mag.*, vol.2, no.2, pp.78–83, June 2018.
- [12] T. Nguyen, Q. Pham, V. Nguyen, J. Lee, and Y. Kim, "Resource allocation for energy efficiency in OFDMA-enabled WPCN," *IEEE Wireless Commun. Lett.*, vol.9, no.12, pp.2049–2053, Dec. 2020.
- [13] X. Zhou, C.K. Ho, and R. Zhang, "Wireless power meets energy harvesting: A joint energy allocation approach in OFDM-based system," *IEEE Trans. Wireless Commun.*, vol.15, no.5, pp.3481–3491, May 2016.
- [14] F. Wang and X. Zhang, "Resource allocation for wireless power transmission enabled full-duplex OFDMA mobile wireless networks," *Proc. IEEE Global Commun. Conf. (GLOBECOM)*, Abu Dhabi, UAE, pp.1–6, Dec. 2018.
- [15] X. Zhang and F. Wang, "Resource allocation for wireless power transmission over full-duplex OFDMA/NOMA mobile wireless networks," *IEEE J. Sel. Areas Commun.*, vol.37, no.2, pp.327–344, Feb. 2019.
- [16] Y. Zeng and R. Zhang, "Optimized training for net energy maximization in multi-antenna wireless energy transfer over frequency-selective channel," *IEEE Trans. Commun.*, vol.63, no.6, pp.2360–2373, June 2015.
- [17] N. Lee, H.J. Yang, and J. Chun, "Achievable sum-rate maximizing AF relay beamforming scheme in two-way relay channels," *Proc. IEEE Int. Conf. Commun. Workshops*, Beijing, May 2008.
- [18] H.H. Kha, H.D. Tuan, and H.H. Nguyen, "Fast global optimal power allocation in wireless networks by local D.C. programming," *IEEE Trans. Wireless Commun.*, vol.11, no.2, pp.510–515, Feb. 2012.
- [19] S. Diamond and S. Boyd, "CVXPY: A python-embedded modeling language for convex optimization," *J. Machine Learning Research*, vol.17, pp.2909–2913, 2016.
- [20] C.Y. Ng and C.W. Sung, "Low complexity subcarrier and power allocation for utility maximization in uplink OFDMA systems," *IEEE Trans. Wireless Commun.*, vol.7, no.5, pp.1667–1675, May 2008.
- [21] X. Lu, P. Wang, D. Niyato, D.I. Kim, and Z. Han, "Wireless networks with RF energy harvesting: A contemporary survey," *IEEE Commun. Surveys Tuts.*, vol.17, no.2, pp.757–789, 2nd Quart., 2015.
- [22] FCC Rules and Regulations Part 15 Section 247, Operation within the bands 902–928 MHz, 2400–2483.5 MHz, and 5725–5850 MHz.



Keigo Hirashima received the B.Eng. degree in electrical and electronic engineering from Ibaraki University, Hitachi, Japan in 2022. He is currently a M.Eng. candidate at Ibaraki University. His research interests include signal processing for wireless communications.



Teruyuki Miyajima received B.Eng., M.Eng., and Ph.D. in electrical engineering from Saitama University, Saitama, Japan, in 1989, 1991, and 1994, respectively. In 1994, he joined Ibaraki University, Hitachi, Japan, where he is currently a professor in the domain of electrical and electronic systems engineering. His current interests include signal processing for wireless communications. Dr. Miyajima is an IEEE member.